PHYSICAL REVIEW B VOLUME 32, NUMBER 10 15 NOVEMBER 1985

Electronic structure of ferromagnetic iron: Fermi surface

Tashi Nautiyal
Physics Department, University of Lucknow, Lucknow-226007, India

Sushil Auluck
Physics Department, University of Roorkee, Roorkee-247667, India
(Received 6 July 1984; revised manuscript received 22 October 1984)

A Fermi-surface model is developed for ferromagnetic iron based on the interpolation scheme of Baker and Smith for bcc transition metals. A reasonably good Fermi surface is obtained. We present theoretical results on interference orbits. These results are found to be encouraging upon comparison with the experimental data of Coleman *et al.*

I. INTRODUCTION

Iron is one of the metals for which band-structure calculations were performed as early as the 1940's. This metal is of particular interest because it exhibits ferromagnetism [below its Curie temperature (770 °C)[1]]. Iron has been the subject of a long series of calculations employing a variety of techniques.[2–12] Despite all this work on it, iron still presents a formidable challenge in that its Fermi-surface topology is still a matter of controversy.[13] The agreement between the calculated and the experimental Fermi surface in the case of iron is not as good as for other transition metals. In addition, the Fermi surface of iron, being very complex, hosts a number of interference orbits[14] accounting for additional frequencies [absent in de Haas–van Alphen (dHvA) experiments] observed recently in magnetoresistance oscillations.[15] These orbits have not been discussed in any of the theoretical models so far. These features of ferromagnetic iron make it a fascinating subject of study.

We have constructed here an optimal representation of the electronic band structure of ferromagnetic iron using an interpolation scheme which is based on the experimental results of dHvA measurements.[16,17] The success of the interpolation scheme in the case of ferromagnetic nickel[18] and other transition metals[19,20] encourages us to adopt this line of approach. To start with, we make use of the band structure of paramagnetic iron using the interpolation scheme of Baker and Smith[21] for bcc transition metals. The parameters for paramagnetic iron were obtained[21] by fitting the augmented-plane-wave calculations of Wood.[22] We arrive at the band structure of ferromagnetic iron by introducing the exchange interaction and the spin-orbit coupling which play a significant role in ferromagnetic iron. In our earlier work,[23] we have already seen that this starting set of parameters[21] gives a fairly good representation for the optical properties of iron.

The main reason why we resorted to this set of parameters for paramagnetic iron[21] is as follows. First-principles calculations, even with the neglect of exchange interaction and spin-orbit coupling, are very complicated. Though Callaway and co-workers[2,3] have presented self-consistent-field calculations with inclusion of the exchange potential for ferromagnetic iron, their work does not give an accurate representation of the Fermi-surface orbit areas, and hence we could not use their band structure to obtain a good guess at the interpolation-scheme parameters. Also the ambiguities associated with the Fermi surface (FS) and, therefore, with the band structure of the ferromagnetic iron discourage any effort to obtain the interpolation-scheme parameters straightway for the ferromagnetic iron.

Since the dHvA experiments are very accurate, we have adopted an approach that relies on dHvA data to obtain an optimal set of interpolation-scheme parameters (see Table I). We fitted those Fermi-surface orbit areas which are well identified. This helps us in arriving at an energy-band structure that yields a good fit to the experimental Fermi-surface data on ferromagnetic iron. In this paper we report the Fermi surface we obtain by fitting some of the extremal orbits and present our results on the interference orbits.

II. PARAMETRIZATION OF THE FERMI SURFACE

The extremal areas are found by numerical integration of the Fermi radii calculated at a fixed interval of rotation in the plane normal to the direction (θ,ϕ) of the applied magnetic field. The integration formula used by Lee,[24]

$$\delta A = [\tfrac{1}{2}(r_1^2 + r_2^2)]\tfrac{1}{2}\delta\psi \ , \tag{1}$$

has been made use of, where δA is the area of a sector bounded by radii r_1 and r_2, and $\delta\psi$ is the vertex angle of the sector. The calculation of the extremal areas is simplified by the symmetry considerations.

We considered 16 orbits for the purpose of fixing the band-structure parameters. We changed the band-structure parameters and calculated the FS orbit areas. Simultaneously the band mass m_b was calculated in order to get an estimate of the extreme error ΔE_F [Eq. (5)]. The job was not simple owing to the nonlinear variations in the Fermi-surface orbit areas that changes in each parameter, and combinations of them, produce. This set of parameters provides us with a reasonably good band struc-

TABLE I. Parameters of the interpolation scheme for the empirical band structure of ferromagnetic iron. Energies are in rydbergs. The Fermi energy is 0.76 Ry.

OPW	
α	0.023 14
β	0.106 10
V_{110}	0.105 00
V_{200}	0.157 50
V_{211}	0.000 00
Orthogonality and hybridization	
R	0.505 10
S	1.122 00
B_e	1.273 00
B_t	1.485 00
d bands	
A_1	0.011 452
A_2	−0.000 302
A_3	−0.010 734
A_4	−0.020 500
A_5	0.015 520
A_6	−0.009 748
E_0	0.709 00
Δ	0.007 80
Spin orbit	
ξ	0.0035
Exchange splitting	
E_s	0.0207
E_d	0.1300

ture for ferromagnetic iron. The total Hamiltonian used was

$$H = H_{\text{para}} + H_{\text{SO}} + H_{\text{ex}} , \tag{2}$$

where H_{para} is the Hamiltonian for paramagnetic iron:[21]

$$H_{\text{para}} = \begin{bmatrix} H_{ss} & H_{sd} \\ H_{ds} & H_{dd} \end{bmatrix} . \tag{3}$$

Here subscript s stands for s bands which have been represented by seven orthogonal plane waves.[21] The subscript d stands for the d bands represented by five tight-binding wave functions. H_{SO} is the usual spin-orbit coupling which is a relativistic phenomenon and is included in a manner shown below:[25]

$$H_{\text{rel}} = \begin{bmatrix} H_{ss} & H_{sd} & 0 & 0 \\ H_{ds} & H_{dd}+\xi M & 0 & \xi N \\ 0 & 0 & H_{ss} & H_{sd} \\ 0 & -\xi N^* & H_{ds} & H_{dd}+\xi M \end{bmatrix} . \tag{4}$$

This doubles the dimensions of the model Hamiltonian. The matrices M and N have been taken from the work of Abate and Asdente.[25] ξ is the spin-orbit coupling parameter. The spin-orbit interaction term is included only in the elements between d functions where degeneracy effects are important.

The exchange interaction H_{ex} is taken along the lines of Zornberg.[26] Different exchange splittings were taken for s and d bands since the s bands are known to have very small exchange splitting as compared to the d bands.[18,27]

Since we are calculating the energy eigenvalues by diagonalizing the model Hamiltonian (2), it seems reasonable to express errors in the calculated extremal areas in terms of the shift ΔE_F in the Fermi energy required to bring the calculated Fermi-surface area in agreement with the experimental area. ΔE_F may be expressed as[28]

$$\Delta E_F = \frac{\hbar^2}{2\pi} \frac{\Delta A}{m_b} , \tag{5}$$

where ΔA is the difference in the calculated and the experimental area and m_b is the band mass.

III. RESULTS

A. Fermi-surface extremal orbits

The fit to the Fermi-surface orbit areas of ferromagnetic iron along with the band masses is presented in Table II along with the existing theoretical results.[2,6,10] Also tabulated are the available experimental Fermi-surface orbit areas and the errors for the various theoretical fits in order to give an idea of the degree of accuracy of all the calculations. Our results for the Fermi-surface orbit areas, A's, are in terms of dHvA frequencies f for the orbits since the two are related,

$$A = 2.673 \times 10^{-9} f ,$$

where A is in a.u. and f is in G.

The orbit areas obtained by us show fairly good agreement with the experimental ones for all the orbits, barring the III and VII orbits, for which the results have comparatively larger error. The experimental data for I to VI orbits are from Baraff,[16] for VII from Coleman *et al.*,[15] and for VIII from Lonzarich.[13] The **k** vectors on the Fermi surface, as obtained by us, for various unhybridized Fermi-surface orbits in the symmetry planes (100) and (110) are plotted in Fig. 1(a). Once we take the spin-orbit interaction into account, we are able to trace a Fermi-surface orbit properly hybridized with the orbits that intersect it. The hybridized Fermi-surface sheets are illustrated in Fig. 1(b). Comparison of Fig. 1(a) (with $\xi=0$) and Fig. 1(b) (with $\xi\neq 0$) exemplifies the effect of spin-orbit coupling—the way it hybridizes and changes the nature of bands, thus leading to hybridization of various Fermi-surface sheets. Determination of unhybridized and hybridized Fermi-surface orbit areas helps in straightforward determination of some of the interference-orbit areas.

B. Interference orbits

Interference orbits result when there is a junction of Fermi-surface sheets. At such junctions the propagating electron state is split into a transmitted and a reflected

TABLE II. Fermi-surface data for ferromagnetic iron. The first, second, and third entries in the third through sixth columns are the Fermi-surface area in MG, the band mass, and the extreme error in mRy, respectively. Band masses are not available for Ref. 2. Experimental data for the I–VI orbits are from Baraff (Ref. 16), for VII from Coleman (Ref. 15), and for VIII from Lonzarich (Ref. 13). The experimental masses are from Gold *et al.* (Ref. 17).

Orbit	Experimental		This work			Theory[a]		Theory[b]			Theory[c]		
I (100)	436		430.9	3.13	1.40	412	6.52	432	2.06	1.65	398	2.24	10.32
(110)	349	2.6	348.4	3.27	0.22	310	14.59	348	1.63	0.52	345	1.90	1.50
(111)	370		378.2	2.72	−2.56	373	0.94	368	2.36	0.72			
III (100)	20.6		18.1	−1.13	−1.88	9.4	−8.46	18.6	−1.00	−1.70	5.3	−1.55	−11.55
(110)	33.4		29.0	−1.76	−2.11	15.5	−8.63	29.2	−1.63	−2.19			
(111)	27.0		21.4	1.27	−3.77	12.2	−9.92	23.0	−1.25	−2.72			
IV (100)	15.0		15.5	−0.98	0.43	7.0	−6.97	16.0	−0.87	0.98	4.3	−1.03	−9.32
(110)	12.3		12.7	−0.74	0.50	6.9	−6.19	13.4	−0.71	1.32	3.8	−0.77	−9.75
(111)	11.4		12.6	−0.74	1.40	6.6	−5.56	13.0	−0.70	1.94			
V (100)			238.1	−2.60		248		250	−2.19		226	−2.33	
(110)			165.4	−1.56		180		186	−1.55		169	−1.90	
(111)	157	−1.7	159.3	−1.39	−1.39	155	−1.23	163	−1.16	4.4			
VI (100)	71.0		67.7	2.29	1.23	76	−1.86	72.7	1.91	−0.76			
(110)	58.0		55.0	1.86	1.38	63	−2.75	60.1	1.57	−1.14			
(111)	52.2	2.8	49.5	1.67	1.37	59	−3.46	53.9	1.40	−1.03			
VII (100)	4.2		7.1	0.68	−3.64	5.4	−1.50	3.7	0.31	1.33			
(110)	4.1		6.0	0.51	−3.09	6.1	−3.33	3.8	0.34	0.75			
VIII (100)	1.43		0.62	−0.33	−2.06	16	37.57	1.29	−0.30	−0.40	33	−0.52	81.40
(110)	1.37		1.20	−0.48	−0.30	15.8	25.69	1.11	−0.26	−0.85	49	−0.69	84.78

[a]See Ref. 2.
[b]See Ref. 6.
[c]See Ref. 10.

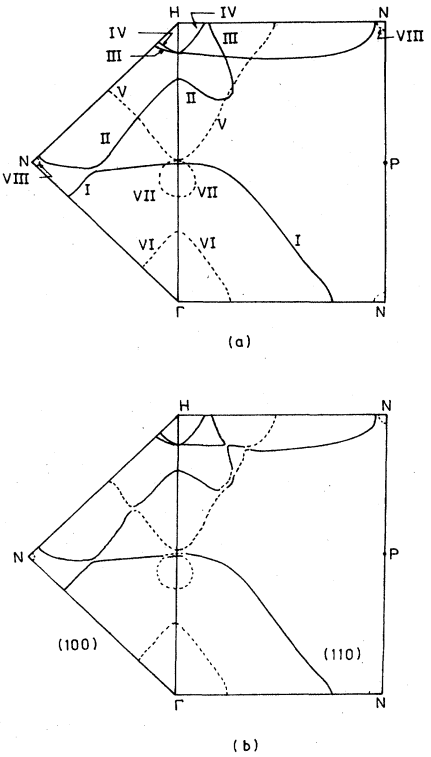

FIG. 1. (a) Unhybridized Fermi-surface sheets of ferromagnetic iron. (b) Hybridized Fermi surface sheets of ferromagnetic iron. Solid (dashed) lines stand for Fermi-surface sheets of majority (minority) carriers.

state. Both of these states propagate along well-defined trajectories, first diverging and then intersecting at a subsequent junction where coherent recombination can take place. Such junctions are characterized by fractional magnetic-breakdown probability.

Our Fermi-surface model (Fig. 1) is capable of giving rise to almost all the possible interference orbits in the (100) and (110) planes of the Brillouin zone. The interference orbit areas can be calculated by making use of the Fermi-surface topology we obtain. The interference orbit frequencies predicted from our model and those obtained experimentally by Coleman *et al.*[15] are listed in Table III. The identification of these, due to Coleman *et al.*,[15] is shown in Fig. 2. These interference orbits arising from various extremal orbits or open orbits are not present in dHvA oscillations associated with closed orbits. Hence, one cannot determine their area through dHvA experiments. These orbits together with dHvA data are helpful in furnishing a better understanding of the Fermi-surface topology.

The first interference orbit comes into the picture from the hybridization of II and V orbits in the (100) plane. Our model gives a value of 24.8 MG for the frequency of this orbit, which has experimentally been predicted to be 22 MG from magnetotransport measurements in iron.[15] The second interference orbit arises from I, II, and V orbits in the (100) plane. Our model estimates its frequency as 12.4 MG against the experimental value of 11 MG. The III and IV majority-carrier Fermi-surface sheets are

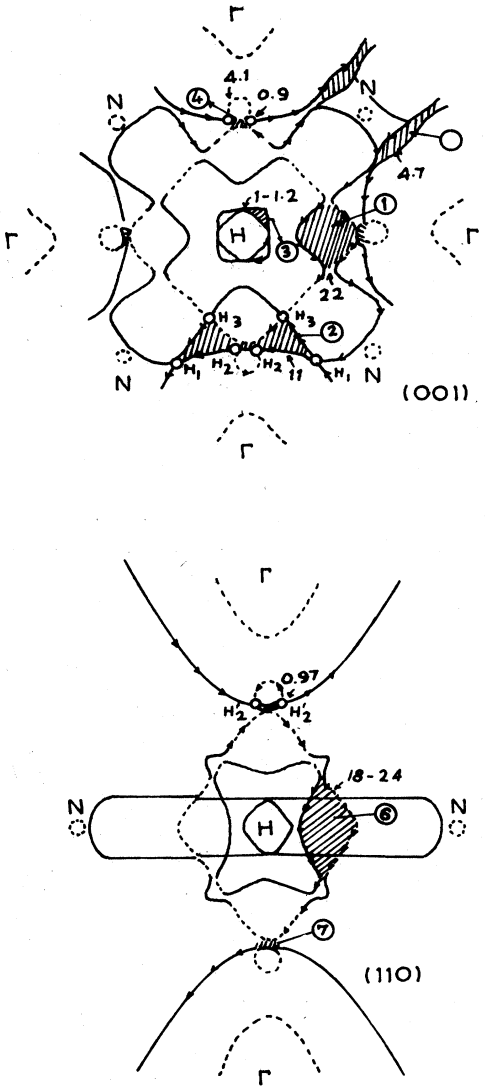

FIG. 2. Possible interference orbits in (100) and (110) planes (Ref. 15).

responsible for the third interference orbit in the (100) plane, for which we obtain a value slightly smaller in magnitude (0.7 MG) than predicted by Coleman *et al.* The reason why we obtain a smaller value is clear from Table II. Our fit to the III (100) orbit is lower than the

TABLE III. Interference orbit areas (in MG).

Orbit	Experiment[a]	This work
1	22	24.8
2	11	12.4
3	1—1.2	0.7
4	0.9	0.6
5	4.7	
6	18—24	13.3
7	0.97	0.2

[a]See Ref. 15.

experimental value, whereas the fit to the IV (100) is quite accurate. A low value for the frequency of the III (100) orbit leads to a smaller frequency for the third orbit. The fourth interference orbit is obtained from the hybridization of majority-carrier Fermi-surface sheet I, centered about Γ, and the minority-electron ball VII along the Δ direction in the (100) plane. We find this orbit to have a frequency of 0.6 MG. Coleman *et al.* predict it to be around 0.9 MG.

The fifth interference orbit with a frequency of 4.7 MG (Ref. 15) is not obtained in our model since the hole arms II get pinched off along the *HN* direction in our model ruling out the possibility of the existence of a fifth interference orbit. Only a Fermi-surface model in which these arms do not get pinched off and are extended along the *HN* direction would give rise to this orbit. Seeing the existing ambiguity in the neighborhood of the *N* point,[13] it is difficult to decide whether these arms should extend along *HN* or get pinched off. Hence, one is not certain whether this is the correct origin or identification of this fifth orbit or should this frequency of 4.7 MG be associated with some other interference orbit.

The sixth interference orbit, which occurs due to the hybridization of II, V, and III orbits in the (110) plane, is found to have a frequency of 13.3 MG. Experimentally, this has been predicted to be in the range 18—24 MG. The seventh interference orbit, arising from the hybridization of I and VII orbits in the (110) plane is found to be very small (0.2 MG) in our model as compared to the experimental value of 0.98 MG. Thus, we observe that our model gives a qualitative estimate for most of the interference orbit frequencies.

IV. CONCLUSIONS

We have presented in this paper the Fermi surface of ferromagnetic iron using the interpolation scheme of Baker and Smith[21] for bcc transition metals. We find that the set of interpolation-scheme parameters obtained by making use of the dHvA data yields fairly good band structure.[29] We obtained a model for the Fermi surface which is in good agreement with the dHvA data. We have, for the first time, presented results on the interference orbits theoretically. We see that the results obtained for these are good and seem to support the assignments given by Coleman *et al.*[15] However, there are still some significant differences between our calculated areas and the measured areas. Our Fermi surface fails to support one interference orbit. Thus, although our Fermi-surface model for ferromagnetic iron proves to be a good one, it needs improvements in terms of the interference orbits.

In another paper we plan to present a detailed study of the band structure and, also, the optical properties of ferromagnetic iron.

ACKNOWLEDGMENTS

Financial support from the University Grants Commission, India, is gratefully acknowledged. The authors also acknowledge the help of the Roorkee University Regional Computer Centre. Ames Laboratory is operated for the U.S. Department of Energy by Iowa State University under Contract No. 2-7405-ENG-82. This work was supported by the Director of Energy Research, U.S. Office of Basic Energy Sciences.

[1]R. M. Bozorth, *Ferromagnetism* (van Nostrand, Princeton, 1951).
[2]J. Callaway and C. S. Wang, Phys. Rev. B **16**, 2095 (1977).
[3]M. Singh, C. S. Wang, and J. Callaway, Phys. Rev. B **11**, 287 (1975).
[4]J. Hubbard and N. W. Dalton, J. Phys. C **1**, 1637 (1968).
[5]D. M. Hum and K. C. Wong, J. Phys. C **2**, 833 (1969).
[6]H. J. F. Jansen and F. M. Mueller, Phys. Rev. B **20**, 1426 (1979); H. J. F. Jansen, Ph.D. thesis, University of Groningen, The Netherlands, 1981.
[7]L. Kleinmann and R. Shurtleff, Phys. Rev. B **4**, 3284 (1971).
[8]L. F. Mattheiss, Phys. Rev. **134**, A970 (1964).
[9]V. P. Shirokovskiy and Z. V. Kulakova, Phys. Met. Metallogr. (USSR) **25**, 20 (1968).
[10]S. Wakoh and J. Yamashita, J. Phys. Soc. Jpn. **21**, 1712 (1966).
[11]K. J. Duff and T. P. Das, Phys. Rev. B **3**, 192 (1971).
[12]V. L. Moruzzi, J. F. Janak, and A. R. Williams, *Calculated Electronic Properties of Metals* (Pergamon, New York, 1978).
[13]G. G. Lonzarich in *Electrons at the Fermi Surface,* edited by M. Springford (Cambridge University Press, Cambridge, 1980).
[14]R. W. Stark and C. B. Friedberg, Phys. Rev. Lett. **26**, 556 (1971); J. Low Temp. Phys. **14**, 111 (1974).
[15]R. V. Coleman, W. H. Lowrey, and J. A. Polo, Jr., Phys. Rev. B **23**, 2491 (1981).
[16]D. R. Baraff, Phys. Rev. B **8**, 3439 (1973).
[17]A. V. Gold, L. Hodges, P. T. Panausis, and D. R. Stone, Int. J. Magn. **2**, 357 (1971).
[18]J. W. D. Connolly, Phys. Rev. **159**, 415 (1967).
[19]A. K. Bordoloi and S. Auluck, Phys. Rev. B **27**, 5116 (1983).
[20]A. K. Bordoloi and S. Auluck, J. Phys. F **13**, 2101 (1983).
[21]S. K. Baker and P. V. Smith, J. Phys. F **7**, 781 (1977).
[22]J. H. Wood, Phys. Rev. **126**, 517 (1962).
[23]T. Nautiyal and S. Auluck, J. Phys. F **13**, 2419 (1983).
[24]M. J. G. Lee, Phys. Rev. **187**, 901 (1969).
[25]E. Abate and M. Asdente, Phys. Rev. **140**, A1303 (1965).
[26]E. I. Zornberg, Phys. Rev. B **1**, 244 (1970).
[27]S. Wakoh, J. Phys. Soc. Jpn. **20**, 1894 (1965).
[28]M. J. G. Lee, Phys. Rev. B **2**, 250 (1970).
[29]T. Nautiyal and S. Auluck (unpublished).